

## Properties and rapid consolidation of binderless nanostructured Ti (C, N) by pulsed current activated sintering

In-Jin Shon<sup>a,\*</sup>, Kwon-Il Na<sup>a</sup>, Hyun-Kuk Park<sup>a</sup>, Sung-Wook Cho<sup>b</sup>, Jae-Won Lim<sup>b</sup> and Wonbaek Kim<sup>b</sup>

<sup>a</sup>Division of Advanced Materials Engineering and the Research Center of Advanced Materials Development, Engineering College, Chonbuk National University, 561-756, Korea

<sup>b</sup>Minerals and Materials Processing Division, Korea Institute of Geoscience, Mining and Materials Resources, Daejeon, Korea

The grain size of Ti (C, N) decreases with an increase in ball milling time. Ti (C, N) nanopowder was fabricated by high energy ball milling for 10 h. The rapid sintering of nanostructured Ti (C, N) hard materials was investigated with pulsed current activated sintering via a heating sintering process. The advantage of this process is that it allows very quick densification to near theoretical density and prohibition of grain growth in nanostructured materials. A dense nanostructured Ti (C, N) hard material with a relative density of up to 98% was produced with simultaneous application of 80 MPa pressure and a pulsed current of 2700 A within 3 minutes. The effect of ball milling time on the sintering behavior, grain size and mechanical properties of binderless Ti (C, N) was investigated.

**Key words:** Rapid sintering, Nanomaterials, Mechanical properties, Milling.

### Introduction

Ti (C, N) is a promising ceramic materials, because the compound exhibit unusual combinations of physical and chemical properties such as high hardness, high melting point and excellent resistance to oxidation [1]. Industrial applications of the compound are in cutting tools and hard coatings. Furthermore, due to their optical, electronic and magnetic properties, the carbides have been used for optical coatings, electrical contacts and diffusion barriers [2]. It is used extensively in cutting tools and abrasive materials in composite with a binder metal, such as Ni. The binder phase has inferior chemical characteristics compared to the carbide or nitride phase. Most notably, corrosion and oxidation occur preferentially in the binder phase [3]. Hence, the development of binderless Ti (C, N) is needed for water jet nozzles, mechanical seals and sliding parts due to their enhanced corrosion resistance and hardness.

Nanocrystalline materials have received much attention as advanced engineering materials with improved physical and mechanical properties [4, 5]. Since nanomaterials possess high strength, high hardness, excellent ductility and toughness, undoubtedly, considerable attention has been paid to the application of nanomaterials [6~8]. In recent days, nanocrystalline powders have been developed by the thermochemical and thermomechanical process named the spray conversion process (SCP), co-

precipitation and high energy milling [9~11]. However, the grain size in sintered materials becomes much larger than that in pre-sintered powders due to the rapid grain growth during a conventional sintering process. So, controlling grain growth during sintering is one of the keys to the commercial success of nanostructured materials. Unconventional sintering techniques, including high-pressure densification, magnetic pulse compaction and shock densification, have been proposed to overcome the problem of grain growth [12-14]. However, these methods have failed to provide fast, reproducible techniques that yield large quantities of high density samples with nanostructured grains.

The pulsed current activated sintering (PCAS) method has recently emerged as an effective technique for sintering and consolidating high temperature materials [15, 16]. PCAS is similar to traditional hot-pressing, but the sample is heated by a pulsed electric current that flows through the sample and a die. This process increases the heating rate (up to 2000 °K minute<sup>-1</sup>) to a degree much higher than that of traditional hot-press sintering.

In this study, we investigated the sintering of Ti (C, N) without the use of a binder by the PCAS method. The goal of this research is to produce nanopowder and dense binderless nanostructured Ti (C, N) hard material. In addition, we also studied the effect of high energy ball milling on the sintering behavior and mechanical properties of binderless Ti (C, N).

### Experimental procedures

The Ti (C, N) powder with a grain size of <1.4 μm and 99% purity used in this research was supplied by

\*Corresponding author:  
Tel : +82-63-270-2381  
Fax: +82-63-270-2386  
E-mail: ijshon@chonbuk.ac.kr

H.C. Starck. The powder was first milled in a high-energy ball mill (Pulverisette-5 planetary mill) at 250 rpm for various times (0, 1, 4, 10 h). Tungsten carbide balls (9 mm in diameter) were used in a sealed cylindrical stainless steel vial under an argon atmosphere. The weight ratio of balls-to-powder was 30 : 1. Milling resulted in a significant reduction in grain size. The grain size of the Ti (C, N) was calculated from the full width at half-maximum (FWHM) of the diffraction peak by Suryanarayana and Grant Norton's formula [17] :

$$B_r (B_{\text{crystalline}} + B_{\text{strain}}) \cos\theta = k\lambda / L + \eta \sin\theta \quad (1)$$

where  $B_r$  is the full width at half-maximum (FWHM) of the diffraction peak after instrumental correction;  $B_{\text{crystalline}}$  and  $B_{\text{strain}}$  are the FWHM caused by small the grain size and internal strain, respectively;  $k$  is a constant (with a value of 0.9);  $\lambda$  is the wavelength of the X-ray radiation;  $L$  and  $\eta$  are grain size and internal strain, respectively; and  $\theta$  is the Bragg angle. The parameters  $B$  and  $B_r$  follow Cauchy's form with the relationship:  $B = B_r + B_s$ , where  $B$  and  $B_s$  are the FWHM of the broadened Bragg peaks and the standard sample's Bragg peaks, respectively.

The powders were placed in a graphite die (outside diameter, 45 mm; inside diameter, 20 mm; height, 40 mm) and then introduced into the pulsed current activated sintering (PCAS) apparatus shown schematically in Fig. 1. The PCAS apparatus includes a 30 kW power supply which provides a pulsed current (on time; 20  $\mu$ s, off time; 10  $\mu$ s) through the sample, and a 50 kN uniaxial load. The system was first evacuated and a uniaxial pressure of 80 MPa was applied. A pulsed current was then activated and maintained until the densification rate was negligible, as indicated by the real-time output of

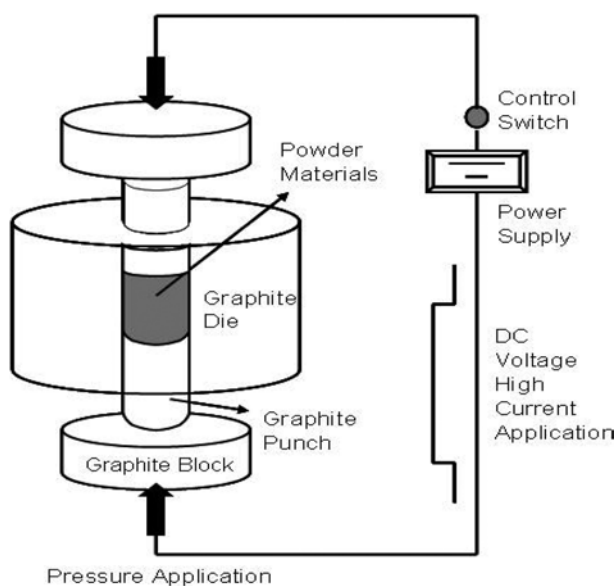


Fig. 1. Schematic diagram of the apparatus for pulsed current activated sintering.

the shrinkage of the sample. The shrinkage was measured by a linear gauge measuring the vertical displacement. Temperatures were measured by a pyrometer focused on the surface of the graphite die. At the end of the process, the induced current was turned off and the sample cooled to room temperature. The process was carried out under a vacuum of  $4 \times 10^{-2}$  Torr (5.33 Pa).

The relative density of the sintered sample was measured by the Archimedes method. Microstructural information was obtained from product samples, which had been polished and etched using Murakami's reagent (10 g potassium ferricyanide, 10 g NaOH, and 100 ml water) for 1-2 minutes at room temperature. Compositional and microstructural analyses of the products were made through X-ray diffraction (XRD), scanning electron microscopy (SEM) with energy dispersive spectroscopy (EDS) and a field emission scanning electron microscope (FE-SEM). Vickers hardness was measured by performing indentations at a load of 10 kg<sub>f</sub> and a dwell time of 15 s.

## Results and discussion

Fig. 2 shows X-ray diffraction patterns of the Ti (C, N) powder after various milling times. The full width at half-maximum (FWHM) of a diffraction peak is wider with milling time due to the strain and the refinement of the powder. SEM images of the (W, Ti)C powder with milling times are shown in Fig. 3. Ti (C, N) powder decreases in size with an increase in the milling time. The grain sizes of Ti (C, N) powder milled for 1, 4, 10 h determined by Suryanarayana and Grant Norton's formula were 180, 40, and 20 nm, respectively. The variations of the shrinkage displacement and temperature with the heating time for a pulsed current 2700A during the sintering of the high energy ball milled Ti (C, N) under a pressure of 80 MPa are shown in Fig. 4. In all cases, the thermal expansion shows as

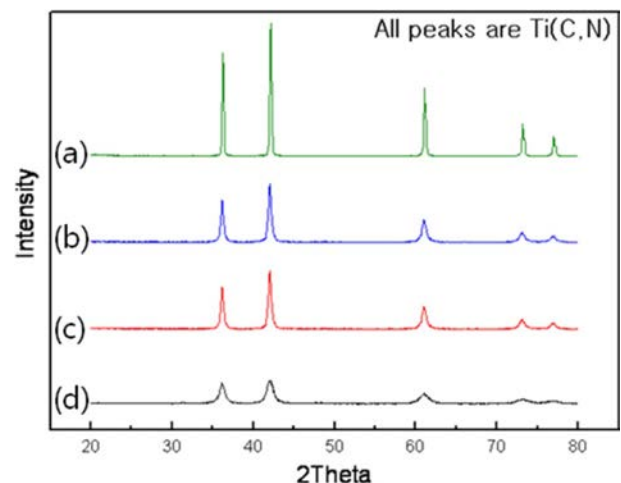


Fig. 2. X-ray diffraction patterns of the Ti (C, N) powder after various milling times : (a) 0, (b) 1, (c) 4, and (d) 10 h.

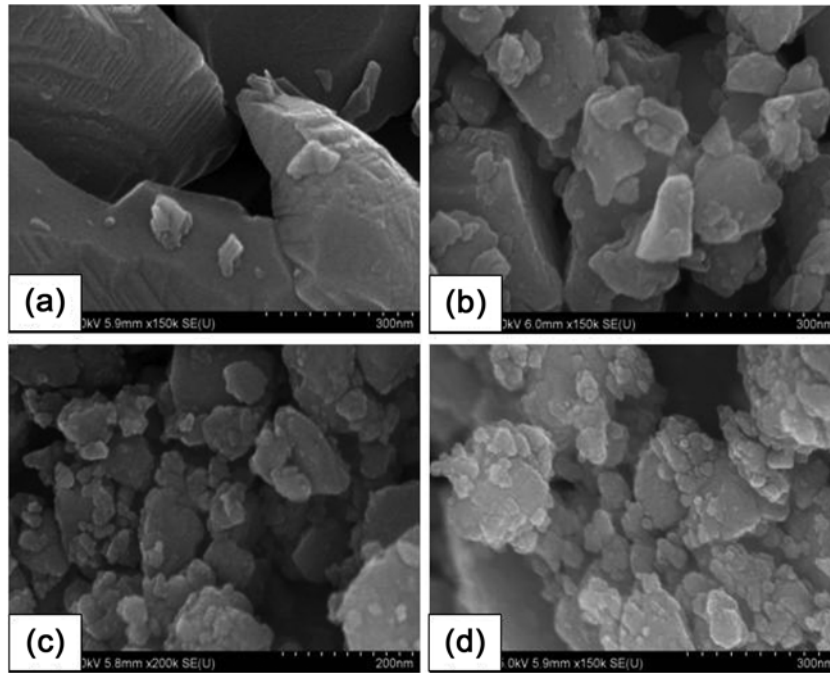


Fig. 3. SEM images of the Ti (C, N) powder after various milling times : (a) 0, (b) 1, (c) 4, and (d) 10 h.

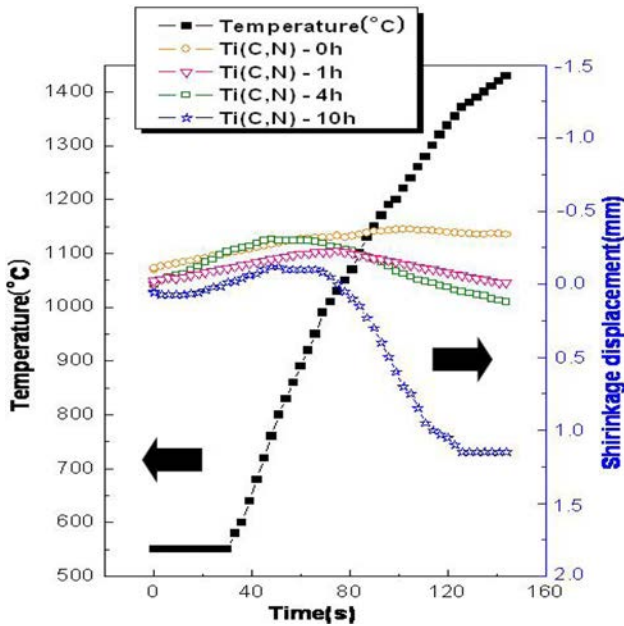


Fig. 4. Variations of temperature and shrinkage with heating time during the pulsed current activated sintering of binderless Ti (C, N) with milling times of 0, 1, 4, and 10 h.

soon as a pulsed current is applied. However, in case of powder milled for 10 h the shrinkage abruptly increases at about 1000 °C. The temperature at which shrinkage started decreased with an increase in the milling time, and the high energy ball milling affected the rate of densification and the final density, as will be discussed below. A high-energy ball milling treatment allows the control of the formation of the compound by fixing the reactant powder microstructure. Indeed, high-energy ball milling produces finer crystallites, more strain and

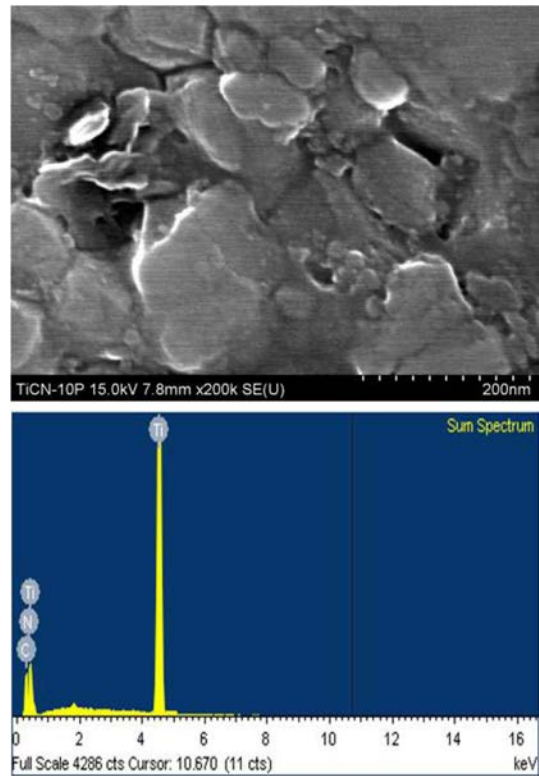
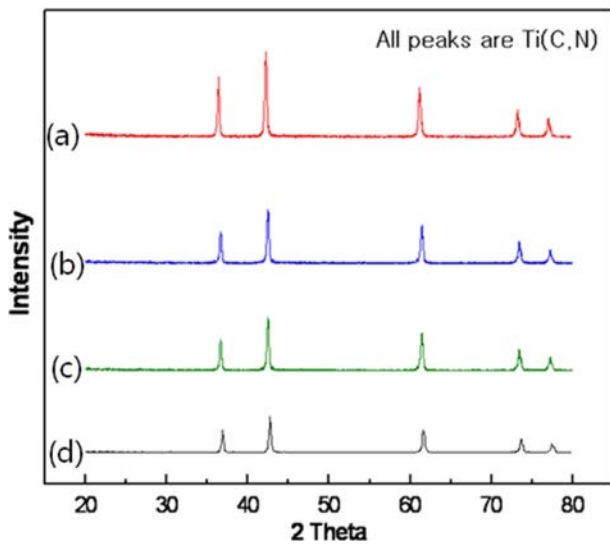


Fig. 5. FE-SEM micrograph of pure Ti (C, N) sintered from the 10 h milled powder.

defects. Therefore, the consolidation temperature decreases with milling time because the driving force for sintering and contact points of powders for atomic diffusion increases. Fig. 5 shows a FE-SEM image of Ti (C, N) sintered from the 10 h milled powder. From the figure, it is known that the Ti (C, N) consists of nanoparticles.



**Fig. 6.** XRD patterns of binderless Ti (C, N) sintered from various milled powders : (a) 0, (b) 1, (c) 4, and (d) 10 h.

And in the EDS spectrum Ti, N and C peaks are detected. Fig. 6 shows the XRD patterns of Ti (C, N) sintered for all four powders used in this study. All peaks are from Ti (C, N).

A plot of  $B_r$  ( $B_{\text{crystalline}} + B_{\text{strain}}$ )  $\cos\theta$  versus  $\sin\theta$  in Suryanarayana and Grant Norton's formula [17] is shown in Fig. 7. The average grain sizes of the Ti (C, N) calculated from the XRD data were about 260, 134, 91 and 77 nm for the samples with milling times of 0, 1, 4, and 10 h and their corresponding densities were

approximately 77, 89, 96 and 98%, respectively. Thus, the average grain size of the sintered Ti (C, N) is not greatly larger than that of the initial powder, indicating the absence of much great grain growth during sintering. This retention of the grain size is attributed to the high heating rate and the relatively short term exposure of the powders to the high temperature.

The role of the current (resistive or inductive) in sintering has been the focus of several attempts aimed at providing an explanation of the observed enhancement of sintering and the improved characteristics of the products. The role played by the current has been variously interpreted, the effect being explained in terms of a rapid heating rate due to Joule heating, the presence of a plasma in pores separating powder particles, and the intrinsic contribution of the current to mass transport [18-21].

Vickers hardness measurements were performed on polished sections of the Ti (C, N) samples using a 10 kg<sub>f</sub> load and a 15 s dwell time. Indentations with large enough loads produced radial cracks emanating from the corners of the indent. The lengths of these cracks permit estimation of the fracture toughness of the materials by means of the expression [22]:

$$K_{IC} = 0.203(c/a)^{-3/2} \cdot H_v \cdot a^{1/2} \quad (2)$$

where  $c$  is the trace length of the crack measured from the center of the indentation,  $a$  is one half of the average length of the two indent diagonals, and  $H_v$  is the hardness.

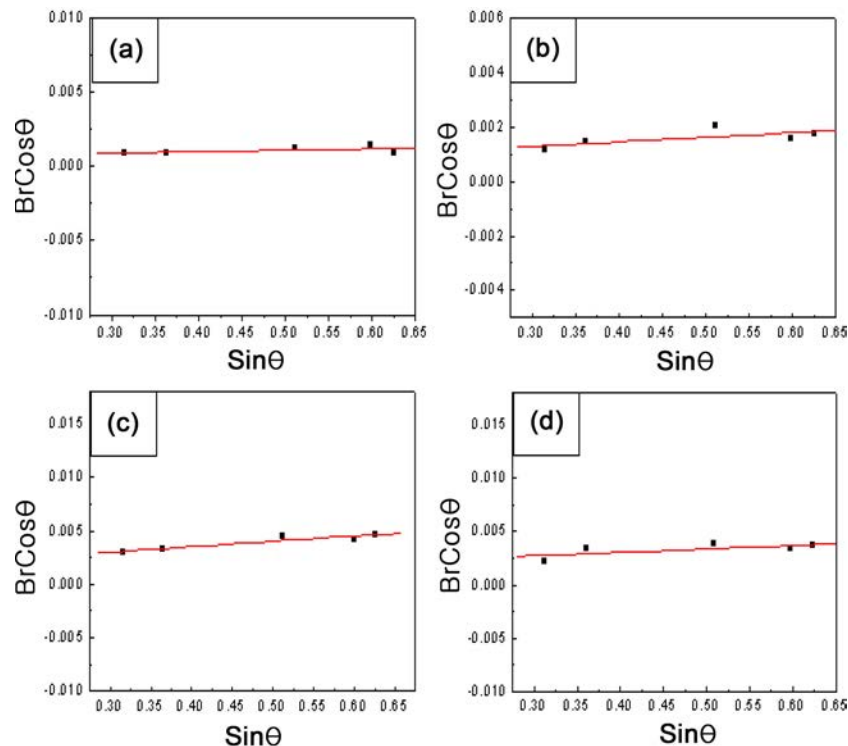


**Fig. 7.** Plots of  $B_r$  ( $B_{\text{crystalline}} + B_{\text{strain}}$ )  $\cos\theta$  versus  $\sin\theta$  for Ti (C, N) sintered from various milled powders : (a) 0, (b) 1, (c) 4, and (d) 10 h.

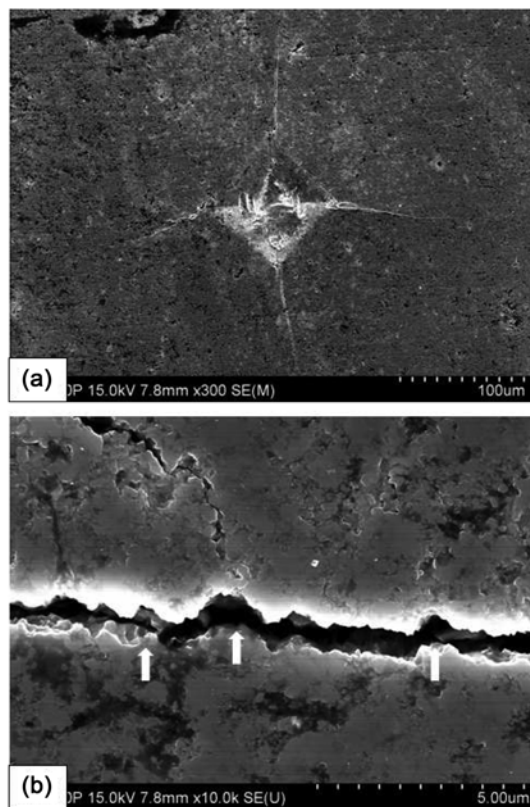


**Fig. 8.** (a) Vickers hardness indentation and (b) median crack propagation in the Ti (C, N) sintered from powder milled for 10 h.

The Vickers hardnesses of the Ti (C, N) with ball milling for 4 and 10 h were  $1550 \text{ kg} \cdot \text{mm}^{-2}$  and  $1960 \text{ kg} \cdot \text{mm}^{-2}$ , and their fracture toughnesses were  $6.2 \text{ MPa} \cdot \text{m}^{1/2}$  and  $6 \text{ MPa} \cdot \text{m}^{1/2}$ , respectively. These values represent the average of five measurements. A higher magnification view of an indentation median crack in the Ti (C, N) is shown in Fig. 8(b), which shows that the crack propagated deflectively ( $\uparrow$ ). The hardness of Ti (C, N) with ball milling for 10 h is very high without a great decrease of the fracture toughness due to refinement of the grains.

### Summary

Nanopowder of Ti (C, N) was fabricated by high energy ball milling. Using the rapid sintering method, PCAS, the densification of binderless Ti (C, N) was accomplished using high energy ball milling. The consolidation temperature decreased with milling time because the driving force for sintering and contact points of powders for atomic diffusion increased. The average grain sizes of the Ti (C, N) were about 260, 134, 91 and 77 nm for the samples with milling times of 0, 1, 4, and 10 h and their corresponding densities were approximately 77, 89, 96 and 98%, respectively. The Vickers hardnesses of the Ti (C, N) with ball milling for 4 and 10 h were  $1550 \text{ kg} \cdot \text{mm}^{-2}$  and  $1960 \text{ kg} \cdot \text{mm}^{-2}$ , and their fracture toughnesses were

$6.2 \text{ MPa} \cdot \text{m}^{1/2}$  and  $6 \text{ MPa} \cdot \text{m}^{1/2}$ , respectively.

### Acknowledgements

This study was supported by a grant from basic research project of the Korea Institute of Geoscience and Mineral Resources and by the Human Resources Development of the Korea Institute of Energy Technology Evaluation and Planning (KETEP) grant funded by the Korea government Ministry of Knowledge Economy (No. 20114030200060).

### References

- O. Yu. Khyzhun, E.A. Zhurakovsky, A.K. Sinelnichenko, V.A. Kolyagin, *J. Electron Spectrosc. Relat. Phenom.* 82, (1996) 179-185.
- S.T. Oyama, *Introduction to the chemistry of transition metal carbides and nitrides in* : S.T. Oyama (Ed.), Blackie Academic and Professional (1996).
- S. Imasato, K. Tokumoto, T. Kitada, and S. Sakaguchi, *Int. J. of Refract. Met. and Hard Mater.* 13 (1995) 305-312.
- H. Suzuki, *Cemented Carbide and Sintered Hard Materials*, Maruzen, Tokyo, (1986).
- M. Sherif El-Eskandarany, *J. Alloys & Compounds* 305, (2000) 225-230.
- L. Fu, L.H. Cao, Y.S. Fan, *Scripta Materialia* 44, (2001) 1061-1065.
- K. Niihara, A. Nikahira, *Advanced structural Inorganic Composite*, Elsevier Scientific Publishing Co., Trieste, Italy, (1990).
- S. Berger, R. Porat, R. Rosen, *Progress in Materials* 42, (1997) 311-322.
- Z. Fang, J.W. Eason, *Int. J. of Refractory Met. & Hard Mater.* 13, (1995) 297-302.
- S.L. Du, S.H. Cho, I.Y. Ko, J.M. Doh, J.K. Yoon, S.W. Park, *I.J. Shon* 49, (2011) 231-236.
- B.R. Kim, K.S. Nam, J.K. Yoon, J.M. Doh, K.T. Lee, I.J. Shon, *J. Ceramic Processing Research* 10, (2009) 171-176.
- S.C. Liao, W.E. Mayo, K.D. Pae, *Acta Mater* 45 (1997) 4027-4032.
- Z.Q. Jin, C. Rockett, J.P. Liu, K. Hokamoto, N.N. Thadhani, *Mater Sci Forum* 465-466 (2004) 93-97.
- V. Ivanov, S. Paranin, V. Khurstov, A. Medvedev, A. Shtolts, *Key Eng Mater* 206-213 (2002) 377-381.
- H.S. Kang, I.Y. Ko, J.K. Yoon, J.M. Doh, K.T. Hong, I.J. Shon, *Metals and Materials International* 17, (2011) 57-62.
- I.Y. Ko, I.J. Shon, J.M. Doh, J.K. Yoon, S.W. Park, N.R. Park, *Journal of Ceramic Processing Research* 12, (2011) 70-73.
- C. Suryanarayana, M. Grant Norton, *X-ray Diffraction A Practical Approach*, Plenum Press, New York, (1998).
- Z. Shen, M. Johnsson, Z. Zhao and M. Nygren, *J. Am. Ceram. Soc.* 85, (2002) 1921-1927.
- J.E. Garay, U. Anselmi-Tamburini, Z.A. Munir, S.C. Glade and P. Asoka-Kumar, *Appl. Phys. Lett.* 85, (2004) 573-577.
- J.R. Friedman, J.E. Garay, U. Anselmi-Tamburini and Z.A. Munir, *Intermetallics*, 12, (2004) 589-596.
- J.E. Garay, J.E. Garay, U. Anselmi-Tamburini and Z.A. Munir, *Acta Mater.*, 51, (2003) 4487-4493.
- K. Niihara, R. Morena, and D.P.H. Hasselman, *J. Mater. Sci. Lett.*, 1, (1982) 12-16.